

Anomalous Transport in Fractured Geologic Media: Basic Physical Models - 11134

Leonid A. Bolshov* **, Igor I. Linge*, Olga A. Dvoretzkaya *, Peter.S. Kondratenko* **,
Leonid V. Matveev*

*Nuclear Safety Institute of Russian Academy of Sciences
52 Bolshaya Tul'skaya St., 115191 Moscow, Russia

**Moscow Institute of Physics and Technology (State University)
9 Institutskii per., Dolgoprudny, 141700 Moscow Region, Russia

ABSTRACT

An overview of the problem of contaminant transport in heterogeneous geological media is given. The main physical principles causing anomalous transport regimes in fractured rock media are identified. Five theoretical models taking into account specific features of geologic media and manifesting non-classical transport behavior are presented and compared with data from field observations.

INTRODUCTION

An extensive amount of field observations accumulated in the last decades evidences that in many cases classical laws can not describe contaminant transport processes in geologic media as discrepancies may be of several orders [1]. In this regard, research of non-classical transport was undertaken at Nuclear Safety Institute of Russian Academy of Sciences (NSI RAS) to describe radionuclide migration processes in fractured rock media. Specific features of fractured rock formations giving rise to anomalous transport were singled out and a number of physical models for anomalous transport taking into account specific features of geologic media and manifesting non-classical transport behavior transport processes in geologic media were developed. Special attention was paid to the analysis of concentration asymptotic structures at far distances from a contaminant source, which is of primary importance for assessment of the reliability of radioactive waste disposal. To perform the study we take advantage of scaling analysis, the Feynman diagram technique developed in [2] and other tools of modern theoretical physics.

The aim of this paper is to give an overview of the most important results obtained in this study. In the next section the main factors causing non-classical transport in geological media are presented. Six further sections are devoted to the basic physical models taking into account specific features of geologic media and manifesting non-classical transport behavior. In the penultimate section, the results are compared with experimental data. Concluding remarks are given in the final section.

MAIN FACTORS DETERMINING ANOMALOUS TRANSPORT IN FRACTURED MEDIA

One of the key factors determining moisture seepage and contaminant transport in geological media is the geometry of the fracture networks. Such systems as a rule can be classified as percolation media. Their characteristics are determined by the connectivity property of their structural elements. These elements are combined into clusters inside of which moisture migration and solute transport are effective, while between separate clusters these processes are weak. Two characteristics of percolation media are most important. The first one is the existence

of a percolation threshold. Below the threshold, there are only finite clusters, and stationary processes of moisture infiltration in the infinite medium are ineffective. Above the percolation threshold, the medium contains an infinite cluster and the transport is not limited with respect to spatial range. The second characteristic of percolation media is the correlation length ξ . Below the percolation threshold, cluster sizes l are in the range $l < \xi$ (the number of clusters with length scale $l \gg \xi$ is exponentially small). In this case, each individual cluster in the scale interval from a certain a , which we call the lower truncation size, to the dimension of the cluster itself has fractal properties (see Ref. [3]). This means that the cluster as a geometric object has not integral but fractal space dimension. On approaching the percolation threshold, the correlation length tends to infinity, $\xi \rightarrow \infty$, and an infinite cluster arises in the medium. Above the percolation threshold the parameter ξ becomes finite again. The percolation medium in this state is fractal at scales $a < l < \xi$, and is statistically homogeneous at scales $l \gg \xi$.

A basic mechanism of tracer transport in fractured rocks is through advection during moisture seepage. Percolation systems of fractures tend to be highly disordered, so solute advection is a random process. Because of the fractal nature of percolation clusters, correlations of the advection velocity are long-ranged (decaying according to a power law). Due to this factor and because advection is a rather fast transport mechanism, it may provide a super-diffusive transport regime [1] with $\gamma > 1/2$ in the relation

$$R(t) \propto t^\gamma \quad (\text{Eq. 1})$$

for the dependence of contaminant plume size on time (remind that $\gamma = 1/2$ corresponds to classical diffusion).

Another important aspect for transport processes in geological media arises from sharply contrasting properties, caused by the presence of a low-permeability matrix. For solute transport through fractures containing moisture, the matrix plays the role of traps and ultimately gives rise to slowing down infiltration and solute transport. Along with this, a percolation cluster has a complicated topological structure, consisting of a backbone and a set of dead ends. The backbone connects remote parts of the cluster, whereas dead ends are connected with the backbone at only one point, remaining isolated from each other and from other domains of the backbone.

Therefore, with respect to infiltration and transport processes, dead ends also play the role of traps. They together with the matrix may be considered as a low-permeable subsystem of the fractured geological medium, in contrast to the connected fractures of the backbone, which form a high-permeable subsystem.

With regard to the existence of two contrasting subsystem, all tracer particles may be subdivided into two parts: “active particles,” which are those in the high-permeable subsystem, and “passive particles,” which reside in the low-permeable subsystem. Of primary interest are the active particles because of their high effective mobility. The presence of a low-permeability subsystem has two important consequences. The first one is that the number of active particles will decrease over time, as some of them become trapped. The second consequence of the presence of a low-permeable subsystem is to slow down solute transport, promoting a sub-diffusive transport mode (Ref. [1]) with $\gamma < 1/2$ in (Eq. 1).

One more important factor forming transport processes in geological media is the strong fluctuations of the moisture seepage characteristics (Ref. [1]), that arise due to the random

structure of geological media. The evolution of solute concentrations in space and time depends on the specific location of the initial solute concentration distribution (source region). Therefore, spatial fluctuations of medium characteristics may effectively renormalize the solute source power.

Further we present a number of physical models to describe non-classical contaminant transport in geological media taking into account above listed factors.

RANDOM ADVECTION WITH INFINITE CORRELATION LENGTH ($\xi \rightarrow \infty$)

A basis of the model is the equation for particle concentration $c(\vec{r}, t)$

$$\frac{\partial c}{\partial t} + \nabla(\vec{v}c) = 0 \quad (\text{Eq. 2})$$

The volumetric moisture flux $\vec{v}(\vec{r})$ is a random function of coordinates obeying incompressibility equation $div \vec{v} = 0$ and the condition $\langle \vec{v}(\vec{r}) \rangle = 0$, where $\langle \dots \rangle$ is the average over an ensemble of realizations. Flux correlations at large distances decrease according to the power law and the n -point correlation function defined by the equality

$$K_{i_1 i_2 \dots i_n}(\vec{r}_1, \vec{r}_2 \dots \vec{r}_n) = \langle v_{i_1}(\vec{r}_1) v_{i_2}(\vec{r}_2) \dots v_{i_n}(\vec{r}_n) \rangle$$

is a uniform function of the order $-nh$ at $|\vec{r}_i - \vec{r}_j| \gg a$ (for all pairs of \vec{r}_i, \vec{r}_j), where $h > 0$ and a is a short-range truncation radius. In particular, for the pair correlation function we have

$$K_{ij}(\vec{r}_1 - \vec{r}_2) = \langle v_i(\vec{r}_1) v_j(\vec{r}_2) \rangle \sim V^2 (a / |\vec{r}_1 - \vec{r}_2|)^{2h} \quad (\text{Eq. 3})$$

where V is the characteristic value of $K_{ij}(\vec{r}_1 - \vec{r}_2)$ at $|\vec{r}_1 - \vec{r}_2| < a$.

The main results of the analysis of the random advection model (Ref. [4, 5]) consist in the following. At $h > 1$ contaminant transport corresponds to classical diffusion with the diffusivity $D \sim Va$. At $h < 1$ the contaminant concentration averaged over an ensemble of medium realization $\bar{c}(\vec{r}, t) = \langle c(\vec{r}, t) \rangle$ is determined as $\bar{c}(\vec{r}, t) = NR^{-3}(t)\Phi(\zeta)$, $\zeta = r/R(t)$

Here $\Phi(0) \sim 1$ and $\Phi(\zeta) \rightarrow 0$ for $\zeta \rightarrow \infty$; N is the total number of contaminant particles. The quantity $R(t)$, defined as

$$R(t) = (a^h V t)^\gamma \quad \text{with} \quad \gamma = (1+h)^{-1} \quad (\text{Eq. 4})$$

determines the contaminant plume size at time t . Since $\gamma > 1/2$ for $h < 1$, the transport regime under this condition corresponds to the super-diffusion mode.

The asymptotic behavior of concentration at large distances is

$$\bar{c}(\vec{r}, t) \propto \exp(-A \zeta^{(1+h)/h}), \quad A \sim 1 \quad \text{at} \quad r \gg R(t). \quad (\text{Eq. 5})$$

Note that $(1+h)/h > 2$ in the exponent of (Eq. 5) at $h < 1$. Therefore, the concentration decay in the super-diffusion regime of random advection model is of contracted exponential type and is even faster than the Gaussian one in classical diffusion (see Fig. 1). This is in sharp contrast to fractional diffusion (formally a mathematical model based on fractional spatial derivatives), whose tails are of the power-law type.

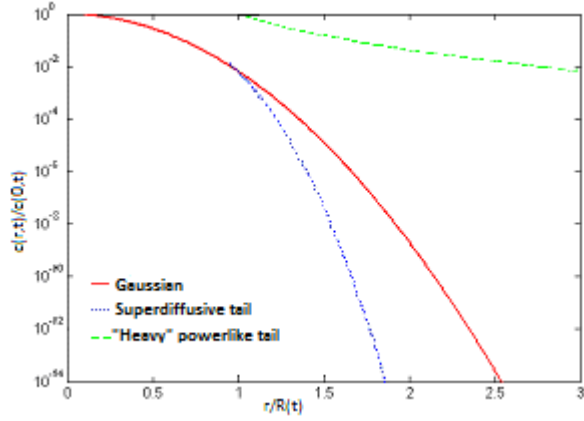


Fig. 1. Gaussian (classical), super-diffusive and “heavy” power-like concentration tails

RANDOM ADVECTION WITH FINITE CORRELATION LENGTH ($\xi < \infty$)

Under the condition of finite correlation length, the advection velocity may be represented in the form

$$\vec{v}(\vec{r}) = \vec{u} + \vec{v}'(\vec{r}), \quad (\text{Eq. 6})$$

where $\vec{u} = \langle \vec{v}(\vec{r}) \rangle$. The correlation function of the “random” term $\vec{v}'(\vec{r})$ possesses the properties of (Eq. 3), which are now valid only at $a \ll |\vec{r}_1 - \vec{r}_2| \ll \xi$. All correlations decay at $|\vec{r}_i - \vec{r}_j| > \xi$ exponentially fast. The main results of the analysis of this model (Ref. [5, 6]) are as follows.

At short times, $t < t_\xi$, where $t_\xi = \xi / u \approx \xi^{1+h} / a^h V$, in the case of $h < 1$, the results reduce to random advection with infinite correlation length (see previous section). At long times, when $t > t_\xi$, the classical diffusive regime is realized:

$$\bar{c}(\vec{r}, t) = N(4\pi D_{eff} t)^{-3/2} \exp\left(-(\vec{r} - \vec{u}t)^2 / 4D_{eff} t\right) \quad \text{with} \quad D_{eff} \sim u\xi. \quad (\text{Eq. 7})$$

This expression is valid at $|\vec{r} - \vec{u}t| \ll ut$.

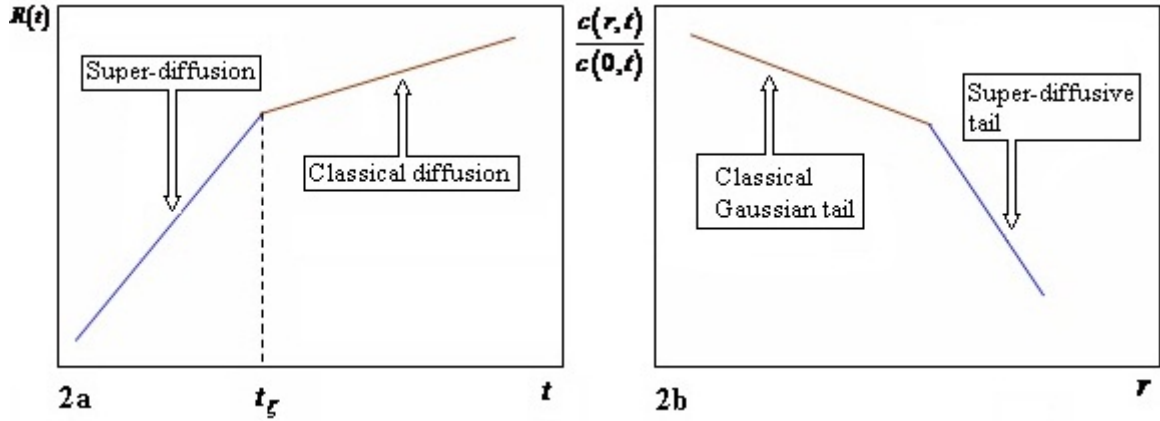


Fig. 2. Contaminant plume size $h < 1$ (2a) and two-stage concentration tail at $t > t_\xi$ (2b)

At large distances $|\bar{r} - \bar{u}t| \gg ut$, the concentration behavior is described by the asymptotic expression (Eq. 7), which also provides the concentration asymptotics at short times for $h < 1$.

Therefore, in the case of finite correlation length, $\xi < \infty$, the concentration tail at $t > t_\xi$ has a two-stage structure. The near stage is the classical one, while the far-tail stage corresponds to superdiffusive asymptotics. The transition between the two stages of asymptotics occurs when

$$\bar{c} \propto \exp\left(-At/t_\xi\right) \quad \text{with} \quad A \sim 1. \quad (\text{Eq. 8})$$

Contaminant plume size at $h < 1$ and two-stage concentration tail at $t > t_\xi$ are represented schematically in Fig. 2.

REGULAR HETEROGENEOUS MEDIUM WITH SHARPLY CONTRASTING PROPERTIES

We consider contaminant transport in a highly contrasting heterogeneous system consisting of a high permeability medium (medium I) with diffusivity D and a low-permeability medium (medium II) with diffusivity d such that $D \gg d$ which was first studied by Dykhne [7]; for this reason later it was called the Dykhne's model [8].

Contaminant transport in the highly permeable medium is governed by the advection–diffusion equation

$$\frac{\partial n}{\partial t} + \bar{u}\nabla n = D\Delta n \quad (\text{Eq. 9})$$

where \bar{u} is the advection velocity and n is the concentration of active particles (those located in medium I). Contaminant transport in the low-permeability medium is governed by the classical diffusion equation for the concentration c of particles in that medium:

$$\frac{\partial c}{\partial t} = d\Delta c \quad (\text{Eq. 10})$$

We use standard boundary conditions of continuity for the concentration and normal flux of particles.

Transport regimes in such a system depend on the geometry of the highly permeable medium and on relations between parameters describing migration properties. We consider two examples of the highly permeable medium: a plain-parallel layer of thickness a , and a straight cylinder (not necessarily a circular one) of cross-sectional area $S \sim a^2$ (see Fig. 3).

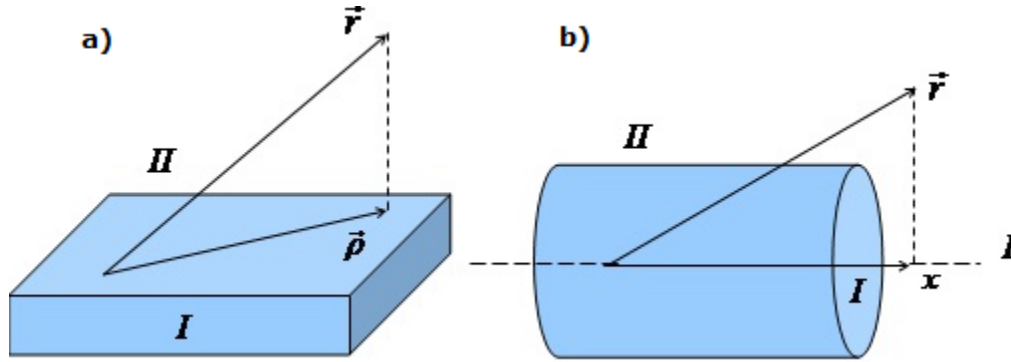


Fig. 3. Two geometric configurations of highly permeable medium: a) a plain-parallel layer, and b) a straight cylinder.

Two characteristic times t_1 and t_u defined by

$$t_u = \frac{4D}{u^2} \text{ and } t_1 = \frac{a^2}{4d}, \quad (\text{Eq. 11})$$

as well as the degree of the medium contrast D/d determines the behavior of the system.

Plane-parallel layer.

1) For $t_u \gg t_1$ D/d the behavior of the system is practically independent of advection. Tracer transport occurs in three stages.

On the first stage, for $t \ll t_1$, tracer particles do not leave medium I , so that tracer transport occurs in the regime of classical diffusion:

$$G(\vec{\rho}, t) \cong \frac{1}{4\pi Dt} \exp\left(-\frac{\rho^2}{4Dt}\right) \quad (\text{Eq. 12})$$

where $\vec{\rho}$ is the two-dimensional radius vector in the plane of the layer, and $\rho = |\vec{\rho}|$.

In the interval $t_1 \ll t \ll t_2$ with $t_2 = t_1 \left(\frac{D}{d}\right)^2$, the low-permeability medium acts as a trap for tracer particles, so that the number of active particles decreases with time as

$$N(t) \sim N_0 \sqrt{\frac{t_1}{t}}, \quad (\text{Eq. 13})$$

and the tracer plume size grows with time as

$$R(t) \sim 4D\sqrt{t_1 t}. \quad (\text{Eq. 14})$$

Therefore, a subdiffusive regime with $\gamma = \frac{1}{4}$ in (Eq. 1) takes place.

For times $t \gg t_2$ the influence of low-permeability medium becomes dominant, so that the transport proceeds in the regime of slow (with diffusivity d) classical diffusion:

$$n(\rho, t) \cong \frac{a}{\sqrt[3]{4\pi dt}} \exp\left(-\frac{\rho^2}{4dt}\right). \quad (\text{Eq. 15})$$

An important feature of the transport is that the change of the regime in time leads to the multi-stage tail structure similar to the case of the finite correlation length in fractal medium (see previous section). For example, for the second time interval, $t_1 \ll t \ll t_2$, when the subdiffusive regime occurs, the nearest tail segment is described by

$$G(\vec{\rho}, t) \cong \frac{1}{2\sqrt{6}\pi Dt} \exp\left\{-3\left(\frac{\eta}{4}\right)^{2/3}\right\}, \text{ with } \eta = \frac{\rho^2}{4D\sqrt{t_1 t}}. \quad (\text{Eq. 16})$$

However, at the distances $\rho \gg \sqrt{Dd/a^2 t}$ concentration dependence (Eq. 16) transforms to (Eq. 12), corresponding to the fast classical diffusion. Similarly, on the stage of the slow classical diffusion (Eq. 15) the nearest tail segment (1.7) changes at distances $\rho \gg d^2 t/Da$ to the dependence (Eq. 16) and then at $\rho \gg \sqrt{Dd/a^2 t}$ to (Eq. 12). This law turns out to be valid for all further cases, so we will not thoroughly describe the tail structure, bearing in mind that it can be easily restored from the time sequence of transport regimes.

2) For $t_1 \ll t_u \ll t_1 D/d$ the following sequence of transport regimes takes place.

In the time intervals $t \ll t_1$ and $t_1 \ll t \ll t_u^2/t_1$ the transport, as before, occurs in the regimes of the fast classical diffusion (Eq. 12) and subdiffusion (Eq. 16), respectively. At times $t \gg t_u^2/t_1$ a new quasi-diffusive regime is formed

$$G(\vec{\rho}, t) \cong \frac{ut_u + 4\rho}{16\pi\sqrt{2D\rho u^3 t_1 t'^3}} \exp\left[-\frac{u\rho}{2D}(1 - \cos\varphi) - \frac{\rho^2}{4D_u t'}\right], \quad (\text{Eq. 17})$$

where φ is the angle between radius-vector $\vec{\rho}$ and the direction of advection velocity \vec{u} ,

$t' = t - \frac{\rho}{u}$, and $D_u = u^2 t_1$. This regime is characterized by the decrease of the total number of active particles, and by a strongly asymmetric concentration profile. The left wing of concentration distribution has the form of power-law train (see also [9]), and the right one is exponentially short.

3) If the advection velocity is large enough, so that $t_u \ll t_1$, the following regimes are realized.

For $t \ll t_u$ the classical two-dimensional fast diffusion occurs transforming in the time interval $t_u \ll t \ll t_3$ into the classical advection diffusion

$$G(\bar{\rho}, t) \cong \frac{1}{4\pi Dt} \exp\left(-\frac{(\bar{\rho} - \bar{u}t)^2}{4Dt}\right). \quad (\text{Eq. 18})$$

For $t \gg t_3$, where $t_3 = (t_u t_1^2)^{1/3}$, the transport is determined by the quasi-diffusion regime (Eq. 17).

Note that in the cases 2) and 3) for the plain-parallel layer the slow diffusion regime (Eq. 15) do not come, as the dispersion due to the transport over medium I , is larger than one due to the regime (Eq. 15).

Now we proceed to the case when high-permeability medium has the form of a straight cylinder.

1) When $t_1 \ln D/d \ll t_u$ the influence of advection can neglected.

At times $t \ll t_1$ the fast classical one-dimensional diffusion occurs

$$G(x, t) = (4\pi Dt)^{-1/2} \exp\left(-\frac{x^2}{4Dt}\right), \quad (\text{Eq. 19})$$

where x is the coordinate along the cylinder axis.

In the time interval $t_1 \ll t \ll \tilde{t}_2$, where $\tilde{t}_2 = t_1 \frac{D}{d} \ln \frac{D}{d}$, logarithmic subdiffusion takes place

$$G'(x, t) \approx \sqrt{\frac{t_1}{t}} \frac{1}{\pi R_1(t)} \left(1 + \frac{x}{R_1(t)}\right) \exp\left(-\frac{x}{R_1(t)}\right), \quad R_1(t) = \sqrt{Dt_1 \ln t/t_1}. \quad (\text{Eq. 20})$$

At $t \gg \tilde{t}_2$ slow subdiffusion occurs (1.7), where one has to put x instead of ρ .

2) If $t_1 \ll t_u \ll t_1 \ln D/d$, then the sequence of regimes is described by (Eq. 19) and (Eq. 20) and

after that in the interval $t_1 \ln D/d \ll t \ll t_{2u}$, where $t_{2u} = t_1 \frac{D_u}{d} \ln^2 \frac{D_u}{d}$, the second logarithmic subdiffusive regime occurs:

$$G'(x, t) \approx \sqrt{\frac{t_1}{t}} \frac{1}{\pi R_2(t)} \left(\frac{ut_u + x}{R_2(t)}\right) \exp\left(-\frac{x}{R_2(t)}\right), \quad R_2(t) = ut_1 \ln t/\tilde{t}_1. \quad (\text{Eq. 21})$$

Ultimately, at $t \gg t_{2u}$, slow classical diffusion (Eq. 15) takes place.

3) For $t_u < t_1$ the sequence of regimes is as follows. Up to the time t_{2u} fast classical one-dimensional diffusion (Eq. 12) and then one-dimensional advection-diffusion

$$G(x, t) \cong (4\pi Dt)^{-1/2} \exp\left\{-\frac{(x - ut)^2}{4Dt}\right\}, \quad (\text{Eq. 22})$$

with the correction in the left wing (in the train)

$$\delta_b G(x, t) \cong \frac{ut_u + 2x}{4u^2} \frac{1}{\sqrt{\pi t_1 t^3}} \quad (\text{Eq. 23})$$

Then the regime of the quasi-diffusion

$$G(x, t') = \frac{x + ut_u/2}{ut'} \frac{1}{\sqrt{4\pi D_u t'}} \exp\left(-\frac{x^2}{4D_u t'}\right), \quad (\text{Eq. 24})$$

and then logarithmic diffusion (Eq. 20) occurs. After that the slow classical diffusion (Eq. 15) is observed.

At times $t \gg t_1$ the number of active particles decreases with time as

$$N(t) \sim N_0 \frac{t_1}{t} \quad (\text{Eq. 25})$$

Note that in the case of the straight cylinder the slow classical diffusion (Eq. 15) is the final transport regime independent of the relation between \tilde{t}_1 and t_u .

CONTAMINANT TRANSPORT OVER PERCOLATION MEDIA WITH CLASSICAL DIFFUSION AS PHYSICAL MECHANISM

Basing on the considerations of the second section, the equation for the concentration of active particles averaged over an ensemble of realizations of the medium can be written as

$$\frac{\partial \bar{c}(\vec{r}, t)}{\partial t} + \int_{-\infty}^t dt' \varphi(t-t') \bar{c}(\vec{r}, t') = D \Delta \bar{c}(\vec{r}, t), \quad (\text{Eq. 26})$$

where D is the bare diffusivity. The kernel $\varphi(t-t')$ has the properties

$$\varphi(t) \sim t_a^{-2} (t/t_a)^{1+\alpha} \quad \text{with } 0 < \alpha < 1 \quad \text{at } t_a \ll t \ll t_\xi, \quad (\text{Eq. 27})$$

$\varphi(t) \sim 1/t_a^2$ at $t \leq t_a$, and $\varphi(t)$ decays exponentially at $t > t_\xi$. Characteristic times t_a and t_ξ are determined by the relations

$$t_a \sim a^2 / D, \quad t_\xi \sim t_a (\xi/a)^{\frac{2}{\alpha}} \quad (\text{Eq. 28})$$

As before, a is the lower truncation size and ξ the correlation length.

In this model, transport regimes and concentration asymptotics for the medium state above the percolation threshold consist in the following (Ref. [7]).

In the interval $t_a \ll t \ll t_\xi$, the transport goes in the sub-diffusive regime with the contaminant plume size given by the relation

$$R(t) \sim a (t/t_a)^{\alpha/2}. \quad (\text{Eq. 29})$$

The total number of active particles (residing in the back-bone of the percolation cluster) decays with time as

$$N(t) \sim N(0)(t_a/t)^{1-\alpha}. \quad (\text{Eq. 30})$$

In this regime, the asymptotic behavior of the concentration at large distances is determined by

$$\bar{c}(\vec{r}, t) \propto \exp(-B\eta^{2/(2-\alpha)}) \quad \eta = r/R(t) \quad B \sim 1. \quad (\text{Eq. 31})$$

Note that the concentration decay in the sub-diffusion regime is slower than the Gaussian one in classical diffusion.

At times $t \gg t_\xi$ the active particle concentration obeys the classical diffusion equation with renormalized diffusivity \tilde{D} :

$$\bar{c}(\vec{r}, t) \cong N_\infty (4\pi\tilde{D}t)^{-3/2} \exp(-r^2/4\tilde{D}t). \quad (\text{Eq. 32})$$

The expression (Eq. 32) is valid at the distances $r < \sqrt{4\tilde{D}t^2/t_\xi}$. If $r > \sqrt{4\tilde{D}t^2/t_\xi}$, then the classical Gaussian tail described by (Eq. 32) changes with the sub-diffusive tail (Eq. 31). So the concentration asymptotics at $t \gg t_\xi$ has the multistage structure.

The total number of active particles at these times remains constant, $N(t) \cong N_\infty$. The renormalization factors for the diffusion coefficient and the total number of active particles are equal:

$$\tilde{D}/D = N_\infty/N(0) = F, \quad F \sim (a/\xi)^{2(1-\alpha)/\alpha}. \quad (\text{Eq. 33})$$

RENORMALIZATION OF CONTAMINANT SOURCE POWER DUE TO FLUCTUATION EFFECTS

If the contaminant source surface area S is comparable to the square of the lower truncation size ($S \sim a^2$), the strong fluctuations of the medium properties renormalize the source power [10]. The renormalization factor K is determined by the rare combinations of favorable conditions – “leakage path“ (punctures). This situation resembles the problem of the tunneling barrier in semiconductors explored in [11], and so we take advantage of the approach of this work. Like [11], the distribution of the puncture concentrations per unit area of the source boundary can be expressed as

$$\rho(u) = (S_0)^{-1} \exp[-\Omega(u)] \quad (\text{Eq. 34})$$

where S_0 is the characteristic cross-sectional size of the puncture, which is small compared to the average distance between punctures, u is an auxiliary variable running the values from 0 to $+\infty$, and $\Omega(u)$ is a function having the properties $\Omega(u) \gg 1$, $\partial\Omega/\partial u < 0$, $\partial^2\Omega/\partial u^2 > 0$.

The analysis [5, 10] using an averaging procedure over the puncture concentration distribution leads to the following results. For large source sizes, $S > a^2$, the renormalizing factor is close to unity. At small source sizes, the renormalizing factor rapidly decreases with S

$$K \propto \exp[-(u_f - u_{opt})] \quad \text{at} \quad S \ll a^2 \quad (\text{Eq. 35})$$

where the quantities u_{opt} and u_f are determined by the equations $(\partial\Omega(u)/\partial u)_{u=u_{opt}} + 1 = 0$ and $(S/S_0)\exp[-\Omega(u_f)] = 1$. Note that we have $K \ll 1$ at $S \ll a^2$.

One additional effect caused by the fluctuations concerns the statistical scatter of the renormalization factor K . The relative scatter $\Delta(K) \equiv (K - \langle K \rangle)^2 / \langle K \rangle$ is small at large source sizes and becomes large at small source sizes.

COMPARISON WITH EXPERIMENT

Non-classical tailing of tracer breakthrough is often observed in pulse injection tracer tests conducted in fractured geologic media. Note that here tailing means long time behavior of the concentration distribution. Usually, researchers associate the non-classical tailing with a diffusive exchange of tracer between mobile fluids traveling through channels in fractures and relatively stagnant fluid between fluid channels, along fracture walls, or within the bulk matrix. However, one series of field tracer tests resulted in breakthrough curves exhibiting strong tailing that could not be explained by diffusive mass exchange [12]. These tests were conducted in a fractured crystalline rock using both a convergent and a weak dipole injection and pumping scheme. Deuterated water, bromide, and pentafluorobenzoic acid were selected as tracers for their wide range in molecular diffusivity. The long time behavior of the normalized breakthrough curves was consistent for all tracers, even when the pumping rate was changed. Hence it follows that the diffusive exchange is not significant in these experiments. So it is reasonable to interpret these tracer results in terms of the random advection model presented in this paper. Taking into account (Eq. 4) and (Eq. 5), we found the interpolation formula described correctly right and left wings of the breakthrough curve:

$$\frac{C(t)}{C_0} = \left(\frac{t_0}{t}\right)^{\frac{3}{1+h}} \exp\left\{-B\left(\frac{t_0}{t}\right)^{\frac{1}{h}}\right\} \quad (\text{Eq. 36})$$

where h and B are fitting parameters.

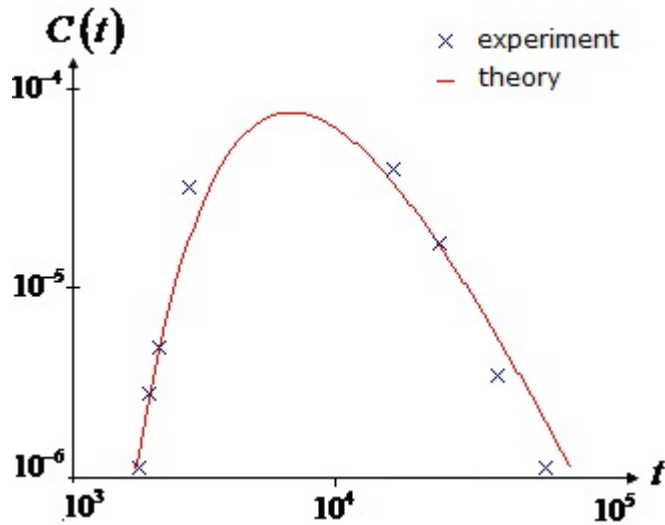


Fig. 4. Theoretical breakthrough curve and experimental data.

The comparison of the prediction given by (Eq. 36) and tracer tests [12] shown in Fig. 4 results in $h \cong 0.4$. Thus super-diffusion behavior is observed. We conclude that agreement between the theory and experiment is quite satisfactory.

CONCLUSIONS

The main results presented in this paper may be summarized as follows.

Four principal structural peculiarities, which may lead to the non-classical radionuclide transport regimes in fractured geological media, are singled out. These are fractal geometry of fractures, advection flows as a dominating transport physical mechanism, sharp contrast in properties distribution, and spatial fluctuations of the medium characteristics.

Super-diffusion behavior of the contaminant concentration is observed in the model of random advection with slow enough decay of the infiltration flux correlations under the condition of the infinite correlation length. In case of finite correlation length contaminant transport goes in the super-diffusion regime at early times and in a classical diffusion at late times.

Depending on time interval, a series of transient transport regimes (among them, sub-diffusion and quasi-diffusion) are revealed in the case of diffusion-advection as transport physical mechanism in regularly heterogeneous contrast media. If the medium contrast is rather sharp, intermediate sub-diffusion or quasi-diffusion may act as a regime which is asymptotic in time.

For diffusion in a percolation dominant medium, being above the percolation threshold, contaminant transport occurs in a sub-diffusion mode at an earlier time and in classical diffusion at later times. In all the models in question, the contaminant concentration decrease at large distances (“in tails”) is of exponential type. It occurs faster in super-diffusion regime and slower in sub-diffusion as compared to the classical (Gaussian) law. None of physical models proves the existence of heavy tails (concentration decay due to power law) peculiar to formal mathematical models of fractional diffusion. The change of transport regimes in time cause the multistage structure of the concentration tails. The current regime determines the stage which is the closest to the contaminant source. Further stages reproduce earlier transport modes in the inverse time order.

Spatial fluctuations of the medium structural properties can lead to the significant renormalization of the contaminant source power. For small source sizes, the renormalizing factor rapidly decreases with contaminant source surface area. One additional effect caused by the fluctuations concerns the statistical scatter of the renormalization factor. It becomes large at small source surface areas.

The results of this study may be used in developing computer codes to assess the reliability of radioactive waste disposals.

Acknowledgments

We acknowledge support from the Russian Foundation for Basic Research (RFBR) under Projects 08-08-01009a, 09-08-00573a, and support from the Federal Target Program “Scientific and academic staff of innovative Russia” for the period 2009-2013 UNDER Contract No. 02.740.11.0746, and support Savannah River Nuclear Solutions, LLC (USA) under Subcontract No. AC81967N.

References

1. L. BOLSHOV, P. KONDRATENKO, K. PRUESS, AND V. SEMENOV, Non-classical Transport Processes in Geologic Media Review of Field and Laboratory Observations and Basic Physical Concepts, *Vadose Zone J.*, Nov 26, 1181-1190 (2008).
2. A.A. ABRIKOSOV and L.P. GOR'KOV, *Sov. Phys. JETP* **8**, 1090 (1958); **9**, 220 (1959).
3. B.B. MANDELBROT, *The Fractal Geometry of Nature*. Freeman, San Francisco, (1982).
4. A. M. DYKHNE, I. L. DRANIKOV, P. S. KONDRATENKO, L. V. MATVEEV, Anomalous diffusion in a self-similar random advection field, *Physical Review E* **72**, 061104 (2005).
5. L. BOLSHOV, P. KONDRATENKO, L. MATVEEV, AND K. PRUESS, Elements of Fractal Generalization of Dual-Porosity Model for Solute Transport in Unsaturated Fractured Rocks, *Vadose Zone J.*, Nov 26, 1198-1206 (2008).
6. P. S. KONDRATENKO, LEONID V. MATVEEV, Random Advection in a Fractal Medium with Finite Correlation Length, *Physical Review E* **75**, 051102 (2007).
7. A. DYKHNE, I. DRANIKOV, P. KONDRATENKO, AND L. MATVEEV, Transport Regimes and Concentration Tails for Classical Diffusion in Heterogeneous Media with Sharply Contrasting Properties, *Vadose Zone J.*, Nov 26, 1191-1197 (2008).
8. O.A. DVORETSKAYA, P.S. KONDRATENKO, AND L.V. MATVEEV, Anomalous Diffusion in Generalized Dykhne Model, *Journal of Experimental and Theoretical Physics*, Vol. 110, No. 1, 58-66 (2010).
9. O. A. DVORETSKAYA AND P. S. KONDRATENKO, Anomalous transport regimes and asymptotic concentration distributions in the presence of advection and diffusion on a comb structure, *Phys. Rev. E* **79**, 41128 (2009).

WM2011 Conference, February 27 - March 3, 2011, Phoenix, AZ

10. L.A. BOLSHOV, A.M. DYKHNE, P.S. KONDRATENKO, Fluctuation Approach to Assessment of the Reliability of Radioactive Waste Disposal, *Journal of Hydraulic Research* 43, No. 2, 208-212 (2005).
11. E.M. RAIKH, AND I. M. RUZIN, Transmittancy fluctuations in randomly non-uniform barriers and incoherent mesoscopics, P.315-368, *In* B. L. Altshuler et al. (ed.) *Mesoscopic Phenomena in Solids*. Elsevier Science Publisher B.V. North-Holland, Amsterdam (1991)
12. M. W. BECKER AND A. M. SHAPIRO, Tracer Transport in Fractured Crystalline Rock: Evidence of Nondiffusive breakthrough Tailing, *Water Resources Research*, Vol. 36, No. 7, 1677-1686 (2000).